

Modelling the geomorphic response to pioneer river engineering works using the CAESAR-Lisflood landscape evolution model

Keiler, Margreth; Coulthard, Tom; Weingartner, Rolf; Zimmermann, Markus; Schürmann, Stefan; Zischg, Andreas Paul; Ramirez, Jorge Alberto

Abstract

Landscape Evolution Models (LEMs) simulate the movement of water and sediment over the landscape. Although much progress has been made in the development of LEMs, few have been tested in rivers subject to anthropogenic impacts that produce high energy flows, transporting large amounts of sediment and causing significant geomorphic changes. As such, it remains uncertain if LEMs are useful and stable under relatively short term 'extreme' geomorphic conditions. To shed light on this topic we use a LEM (CAESAR-Lisflood) and historical documents to develop a detailed reach scale model of the Kander river (Switzerland). This model was used to simulate the unintended impacts of engineering works, occurring in 1714, that deviated the Kander river into a lake and resulted in a large decrease in base level of the river. In 10 years, the model simulates knickpoint propagation that rapidly erodes 2.5 million m³ of sediment and produces a remarkable 27 m of channel erosion. Simultaneously, the model develops the formation of a delta via frequent avulsions. Model testing is performed by comparing model predictions against historical observations of channel incision, knickpoint location, and delta spatial extent. Overall, model error is low and the model remained stable as results do not contain erratic erosion or deposition. Importantly the model suggests that downstream processes occurring at and near the delta have an effect on upstream channel erosion. We also recommend that studies replicating historic landscape changes with LEMs reduce uncertainty in hydrological inputs.

Highlights

- CAESAR-Lisflood replicates the unintended effects of early river engineering works
- CAESAR-Lisflood produces stable output under extreme geomorphic conditions
- Results suggest that downstream processes exert control on upstream erosion

Keywords: landscape evolution model; channel change; knickpoint, river delta, model test, uncertainty

1. Introduction

1.1 Background

Anthropogenic impacts to fluvial systems have been recognized and studied since the nineteenth century onwards (Brown et al., 2017; Gregory, 2006; Hooke, 2000; James and Marcus, 2006; Marsh, 1864). A direct impact are modifications to river morphology aiming at flood hazard reduction, which often have unintended consequences (Benito and Hudson, 2010; Di Baldassarre et al., 2018; Nunnally and Keller, 1979; Wohl, 2006) including alterations to river ecosystems, downstream amplification of flood discharges, reducing sediment transfer or lowering of groundwater levels (Best, 2019; Fortugno et al., 2017; Munoz et al., 2018; Triet et al., 2017). One method to investigate the geomorphic consequences of anthropogenic impacts on rivers is the replication of hillslope and fluvial processes using Landscape Evolution Models (LEMs). LEMs are computer models that simulate the three-dimensional development of landscapes through time using equations to calculate surface water flow and sediment transport (Tucker and Hancock, 2010). LEMs have been applied to anthropogenically modified landforms subject to fluvial erosion. For example, Willgoose and Riley (1998) used the SIBERIA LEM to estimate 1000 years of fluvial sediment transport occurring in uranium mill tailings at a site in Northern Territory, Australia. More recently, Hancock et al. (2019) used SIBERIA to

test the long-term (100-yr) effectiveness of landform designs in stabilizing mining waste undergoing fluvial sediment transport in New South Wales, Australia.

CAESAR-Lisflood (CL) (Coulthard et al., 2013) is a LEM and is the integration of the CAESAR LEM (Coulthard et al., 2002) and the Lisflood-FP hydrodynamic model (Bates et al., 2010; Bates and De Roo, 2000). CL has been frequently used to model geomorphic changes in river reaches (Liu and Coulthard, 2017; Poepl et al., 2019; Ziliani et al., 2020), with recent studies quantitatively verifying CL's capacity to replicate channel changes using observations (Feeney et al., 2020; Pasculli and Audisio, 2015). CL has also been applied in anthropogenically modified landscapes that include rehabilitated mining sites (Lowry et al., 2019) and catchments undergoing forest management (Walsh et al., 2020). However, none of the examples where CL has been tested consider rivers subject to direct human impacts (e.g. engineering works) that produce large movements of sediment in a short period of time (hours to years). As such, it remains uncertain if CL is useful and stable in replicating these extreme geomorphic conditions.

1.2 History of the Kander River

Before 1714, the Kander river flowed into the Aare river at a location that confluences with the Zulg river (Fig. 1 a). During floods, at this confluence the Kander and Zulg rivers transported sediment that subsequently dammed the Aare river and produced backwater effects flooding the city of Thun (Fig. 1 a) (Grosjean, 1962). In particular, the Kander river has been well known for its large sediment yields (Vischer, 2004). Moreover, the sediment input from the Kander forced the Aare river to braid (Vischer, 2004). To reduce the risk of flooding, pioneer engineering works were performed between the years 1711-1714 to deviate the Kander river into Lake Thun (Fig. 1 a).

The first plan for the river deviation was to excavate a channel through the morainic hill of Strättligen with opencast mining methods (Fig. 1 b). The works were interrupted after one year because of the second war of Villmergen. In a second attempt, a tunnel was drilled through the Strättligen hill with a length of 250 m, a width of 12 m, and a height of 4.5 m (Fig. 1 b). The aim of this tunnel was to deviate only flood waters from the Kander river into the lake to make use of the lake's retention capacity to reduce flood peaks. The tunnel was finished in early July of 1714 and the river was partially deviated into the tunnel. However, the bottom of the tunnel unexpectedly eroded quickly and within several days all the Kander's flow was conveyed through the tunnel. Two months after, the tunnel collapsed due to fast incision and lateral erosion and the resulting deviation, called the Kander correction, was produced. In the ensuing years, the new channel in the morainic and underlying older fluvial material proved to be geomorphically unstable and large amounts of erosion occurred within and upstream of the deviated river reach. For example, historical accounts indicate that the Kander correction eroded ~27 m of the riverbed in the first two years since its inception (Koch, 1826; [Wirth et al., 2011](#)). In the lower part of the Kander river, the Kander correction shortened the river course by 8 km and steepened the river gradient from 0.3° to 3.7° (Koch, 1826) (Fig. 1 a). This steepening of the channel increased stream power and bed shear, which contributed to the rapid channel erosion (Wirth et al., 2011).

This human intervention also triggered a cascade of other unintended effects on the hydrological regime and the water management of the Aare river basin. The settlements in the downstream part of the old river course lost their water supply for agriculture. The contribution area of the Lake Thun almost doubled from 1300 km² to 2400 km² from one day to another. Hence, within 24 hours after the Kander

correction, the lake level rose by 20 cm (Bögli, 2018). Thereafter, the city of Thun was flooded in the years 1714, 1715, 1718, 1720, 1721 (Bögli, 2018) by high lake levels and high discharges at the lake's outlet. Due to the higher lake level of Lake Thun the outflow and flow velocity increased remarkably. Consequently, all hydropower facilities along the Aare river in Thun, which were the backbone of the local industry (mill, sawmills etc.), physically collapsed as a result of the high flow velocities and lateral erosion. The lake outflow capacities had to be improved in the following years by excavating and opening a second river course within the city of Thun and stabilizing the shorelines. The management of the unintended consequences has lasted until today; e.g. in the year 2009, nearly 300 years after the human intervention, a bypass tunnel was installed at the outlet of the lake that enables the preventive lowering of the lake level before a predicted large rainfall event in the Aare basin upstream from the lake.

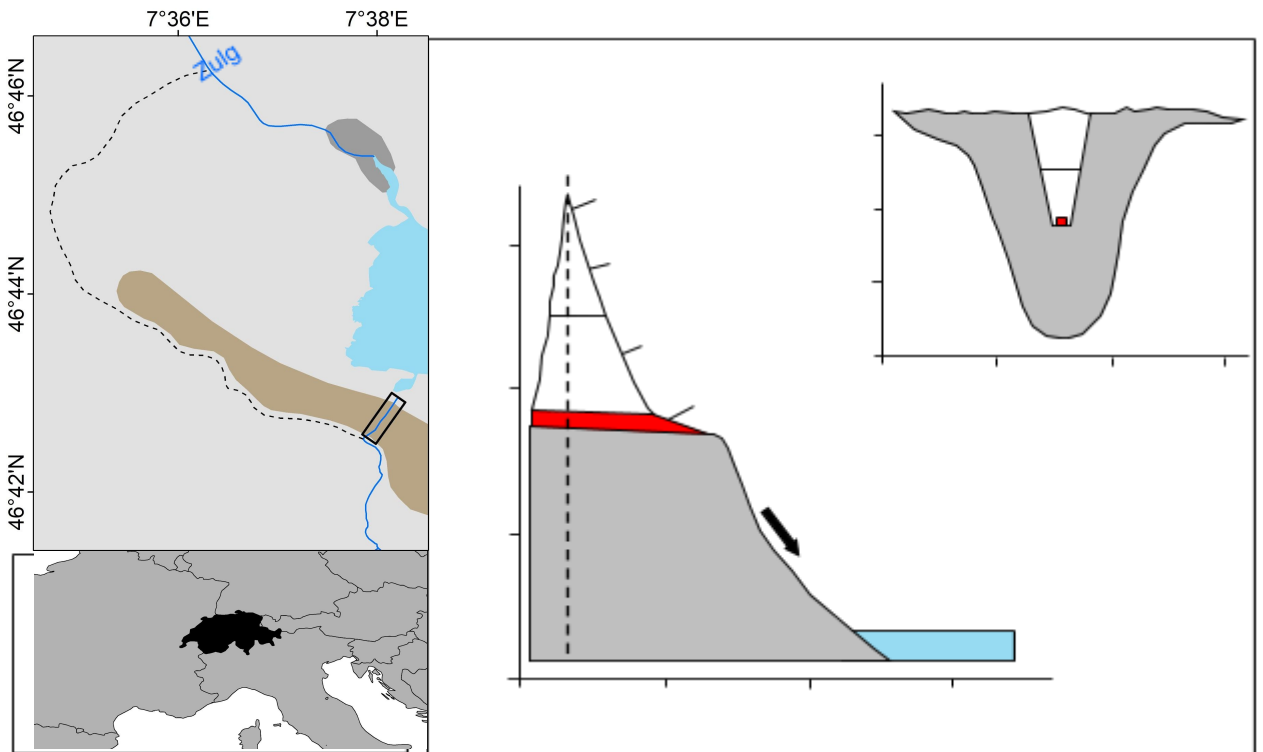
1.3 Study aim

The aim of this paper is to quantitatively test CL on an anthropogenically impacted river reach. To achieve this, we use CL to develop a detailed reach scale model of the Kander river (Switzerland) starting in the year 1714 (Fig. 1 a), and use this model to simulate the extreme geomorphic events that followed engineering works that deviated the Kander river into Lake Thun (Grosjean, 1962; Vischer, 2004; Wirth et al., 2011) (Fig. 1 a). From a geomorphic modelling perspective, the deviation of the Kander river is a unique case because of the large number of historical documents and maps before, during and after the deviations construction (Culmann, 1865; Koch, 1826; Riediger, J.A., 1716; Röthlisberger, 1991; Vischer, 2004). As such, this historical data has allowed us to perform this model test, whereby the Kander correction is a case study of landscape evolution where initial and boundary

conditions are sufficiently constrained, and observations are available for comparison against CAESAR-Lisflood's (CL) predictions.

In this study, we address the following research questions:

- (1) Can CL replicate channel erosion and knickpoint propagation occurring after the deviation of the Kander river?
- (2) Can CL replicate deposition and delta formation after the deviation of the Kander river?
- (3) Does CL remain stable when replicating extreme geomorphic conditions that include the movement of large amounts of sediment in a short period of time?



Lake Thun

Strättligen hill

completed excavation

planned excavation

tunnel

A

flow

550

580

610

640

0

250

500

750

distance (m)

elevation (m)

A

550

580

610

640

0

200

400

600

distance (m)

elevation (m)

[Lake Thun](#)

Thun

[Aare](#)

Kander correction

Strättligen

Kander before 1714

[Kander](#)

N

1 km

a)

b)

c)

200 m



Figure 1. (a) Regional map that includes study area (adapted from Wirth et al. (2011)). Inset indicates location of study (blue dot) in Switzerland (shaded in black). (b) Longitudinal and cross-section of the Kander correction from 1711–1714 (adapted from Vischer (2004)). (c) Historical map of Kander river from 1716 (adapted from Riediger (1716)). Arrows indicate river flow.

2. Methods

2.1 Landscape evolution model

The Landscape Evolution Model (LEM) used is the CAESAR-Lisflood (CL) model (Coulthard et al., 2013). A complete description of CL is described in Coulthard et al. (2013) with a brief summary provided below. CL operates over an initial Digital Elevation Model (DEM) built from a regular grid of cells, and can operate in catchment mode driven by a rainfall time series (Coulthard and Skinner, 2016) or reach mode with point source inputs of water and sediment (as used in this model set up). Water is routed across the DEM and through channels using a quasi 2D flow model based on Lisflood-FP (Bates et al., 2010). Modelled flow velocities are then used to drive sediment transport via a choice of sediment transport equations that operate over nine different grainsizes and can simulate suspended as well as bedload transport. Vertical (e.g. stratigraphic) changes in sediment size are stored

via an active layer system; a comprehensive description of this process can be found in Van De Wiel et al (2007). Further components in CL simulate slope processes enabling the collapse of banks or material added laterally. The erosion and deposition of sediment via the approach above leads to changes in elevation of DEM cells thus simulating morphological changes and how the landscape evolves.

CL simplifies some components of open channel flow simulation (e.g. full inertia) compared to other two dimensional flow models, but this simplification enables it to run much faster allowing smaller grid cells to be used or a larger area to be simulated. Moreover, using CL allows us to model every event and low flow during this period with no need to pick or rely on using only certain events that other approaches may require. The Kander reach simulated here is simple and may well lend itself to even 1D morphodynamic modelling approaches, however this would not allow us to simulate the depositional fan in the lake below the reach, which CL enables. CL is freely available and since 1996 there have been over 60 published studies using the model over a wide range of temporal and spatial scales. In this study we used CL v 1.9.

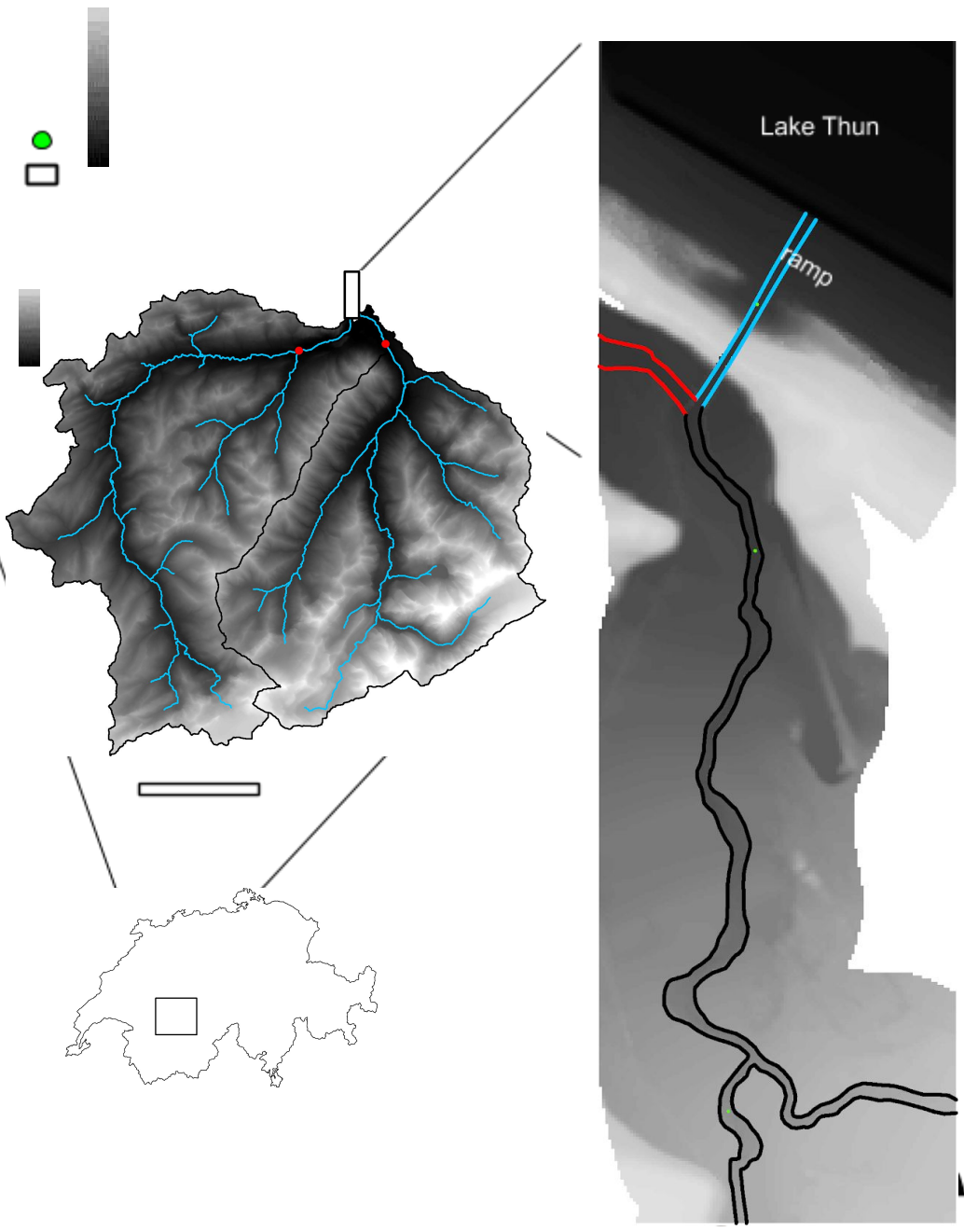
2.2 Reconstruction of the historical digital elevation model

A fundamental requirement for simulating the Kander correction is a hydraulically correct DEM for the past channel and surrounding area. Herein we describe our method to reconstruct a historic DEM using the present-day high-resolution DEM and historic maps. According to the analysis of the remaining geomorphological signatures of the historical riverbed, the Kander river flowed through alluvial sediments with an average inclination of 0.5% and a nearly planar to slightly convex landform before its deviation (c.f. *“Kander before 1714”* and *“Kander”* river reach in

Fig. 1 a). Along the flow line, the original river course had a constant slope over the study area. To reconstruct the original landscape within the modeled area shown in Fig. 2 b, we filled the eroded river channel (of the post-correction DEM; KAWA, 2015) until the original slope and curvature of the overall alluvial fan was restored according to the characteristics of the undisturbed morphology of the adjacent areas. The following detailed procedure was applied to reconstruct the historical DEM. Areas that were geomorphically altered by the river erosion following the deviation of the river were mapped on the post-correction DEM. These areas are confined by the upper lateral crests of the river gorge which deeply incised into the alluvial deposits. In addition, we also mapped the hydraulically relevant manmade features in the landscape that could alter the water flow in the reconstructed DEM (e.g. the structural engineering works related to the highway passing through the study area). Next, anthropogenically modified features were deleted from a DEM with a spatial resolution of 0.5 m (KAWA, 2015) and contour lines derived from the DEM (0.5 m isolines). This results in a DEM with no data values in anthropogenically modified areas and contour line features with voids in those areas. Afterwards, we manually connected the contour lines ending at the left and right lateral borders of the void areas by conserving the adjacent fan slope and planar/longitudinal curvature. Digitized contour lines were then interpolated into a surface representing the alluvial fan in the erased areas of the DEM. This interpolated surface was merged with the present-day DEM and thus the erased anthropogenically modified areas in the DEM could be filled with the interpolated surface of the original geomorphology of the alluvial fan.

This DEM was resampled to a spatial resolution of 10 m to reduce the computation time for modelling, but still adequately represent the channel gradient and planform

of the finer spatial resolution DEM. To replicate the historic channel in the DEM, the river planform was digitized from the earliest available map that was based on topographic surveys in 1868 (post-correction) combined with the geomorphic records of the old riverbed downstream of the correction that are still visible in the present-day DEM. Next, we overlaid the digitized polygon of the historic river course on the reconstructed DEM and assimilated the river planform into the DEM as proposed by Zischg et al. (2018). The historic riverbed was incised into the reconstructed DEM with a depth corresponding to the river conveyance capability of a flood event occurring statistically every two years according to Bhuyian et al. (2017). This flood event corresponds to a present-day discharge of $128 \text{ m}^3 \text{ s}^{-1}$ for the Kander river and $140 \text{ m}^3 \text{ s}^{-1}$ for the Simme river (FOEN, 2020). On average across the whole river reach, the riverbed was initially incised by 2.45 m (river width of 30 m). Iteratively, this incision was corrected locally by simulating the mentioned flood magnitude and heightening or lowering raster cells to meet the target conveyance capacity over the whole reach. Finally, the reconstructed DEM resulted in a pre-correction DEM of the simulation domain without anthropogenic impacts (Fig. 2 b). The interim stages of the reconstruction of the pre-correction DEM are illustrated in Figure S1 a-f.



Simme
 Kander
 N
 500 m
 10 km
 592 3692

 elevation (m)

Kander

corr. tunnel

a)

800

556

elevation (m)

sediment & water input

channel

pre correction

post correction

river reach

gauging station

catchment boundary

obs. channel elevation

Switzerland

obs. knickpoint

Figure 2. (a) Simme and Kander catchments upstream from the (b) simulated reach containing the Kander correction.

2.3 Boundary conditions and initial conditions

Grain sizes for the Kander and Simme river reaches were determined through field measurements summarized in technical reports (Tiefbauamt des Kantons Bern, 2004). Near the confluence, both the Kander and Simme rivers have similar grain size distributions, so the grain sizes of the Kander were applied to the entire reach. In total six grain size classes from silt to boulder were modelled (Fig. S2 a), and each grid cell in the model initially contained the same grain size percentages. The smallest grain size, silt, was modelled as suspended sediment with a fall velocity of 0.00174 m s^{-1} (Ponce, 1989).

a)

b)

c)

d)

The Kander correction drains the Simme and Kander Alpine watersheds (Fig. 2 a) with a combined area of 1094 km², an altitudinal range of 558-3675 m a.s.l., and landcover consisting of 4% glaciers, 23% forest, and 46% grass. For this watershed no discharge records exist during the time of the Kander correction, but historical documents indicate no occurrence of major floods and severe flood damage in the Kander catchment during the 10 years following the construction of the Kander correction (Bütschi, 2008; Röthlisberger, 1991). To drive our simulations, based on these information, we selected contemporary discharges that similarly do not major major flood events. Ten years of hourly discharge (1986-1996) (Fig S3 a, b) were acquired for both the Simme (Simme-Latterbach station) and Kander (Kander-Hondrich station) rivers (Fig. 2 a) and within this record the combined discharge from the Simme and Kander did not exceed discharges with a return period of ten years (313 m³ s⁻¹). Therefore, we assume the selected contemporary discharge and unknown historical discharge have similar magnitudes and variability. Discharge was added to the model at locations upstream from the confluence of the rivers (Fig. 2 b). Flow duration curves (Zambrano-Bigiarini, 2012) were derived using the hourly discharge from both rivers and high-flows, where 20% of time that flow is equaled or exceeded, were estimated to be $\geq 30 \text{ m}^3 \text{ s}^{-1}$ (Fig. S2 b). We assumed that upstream sediment transport mostly occurred in high-flow conditions and only added sediment to the modelled river reach above this threshold (Fig. S3 c, d). The quantity of sediment transported from each river is an annual estimate that was determined through calibration (see below). A portion of this annual amount of sediment was added to each reach every hour and the quantity of sediment added was linearly proportional to the hourly discharge per annum. Moreover, the sediment added to the model consisted of the grain size percentages described earlier.

For initial conditions, we assumed that prior to the correction the Kander and Simme channels were neither significantly incising nor aggrading (i.e. in dynamic equilibrium). Thus, quantities of sediment added to the model should not produce large amounts of erosion and deposition. Model annual sediment inputs were manually calibrated for the Simme and Kander rivers by developing a model without the Kander correction and the original course of the Kander river (Fig. 2 b). This model used the Wilcock and Crowe sediment transport formula (Wilcock and Crowe, 2003). Simulations were run for three years using discharges from 1986-1989 (both Kander and Simme) and tried possible annual total sediment yields within range of published estimates (86,000-155,000 m³ yr⁻¹) (Hinderer, 2001; Schlunegger and Hinderer, 2003). Twenty-four percent and 76% of the sediment supply was added to the Simme and Kander reaches respectively and these proportions were determined from present-day estimates of sediment entering lake Thun (Wirth et al., 2011). Pseudo-equilibrium in the model was determined by 1) calculating whether the sediment added to the model is equivalent to the sediment exiting the model, and 2) whether no discernable change occurs in the reach's channel elevations. Over the three-year simulation annual sediment inputs of 20,000 m³ yr⁻¹ for the Simme and 63,333 m³ yr⁻¹ for the Kander produced relatively stable geomorphic conditions. Comparison of annual channel elevation change (Fig. S2 c) indicated a stabilization of the channel occurring in the third year, with an average channel change of 0.04 m and standard deviation of 0.09 m. Likewise in the third year of simulation the difference between the sediment added and exiting the reach over time is minimal (RMSE = 8 m³ yr⁻¹) (Fig. S2 d). Total calibrated sediment inputs for the model were 83,333 m³ yr⁻¹ and similar to sediment yields estimated for the combined Simme and Kander (86,000 m³ yr⁻¹) using field methods (Hinderer, 2001). Calibrated annual

sediment totals were used for the 10 years of simulation after the Kander deviation. Moreover, at the conclusion of the calibration period the DEM and grainsize proportions per raster cell were saved and represented initial conditions for the remaining simulations.

a)

b)

c)

d)

time (years)

discharge ($\text{m}^3 \text{s}^{-1}$)

sediment ($\text{m}^3 \text{hr}^{-1}$)

Kander

Simme

Kander

From historical documents, summarized by Vischer (2004), the location, elevation (599-596 m), and dimensions (340 m in length, 32 m in width and a slope of 0.46°) of the Kander correction were determined (Fig. 1 b). Using this information, in a geographical information system a linear plane was created representing the Kander correction and mosaicked into the DEM representing initial conditions for the Simme and Kander reach (Fig. 2 b). Downstream from the correction a 248 m long ramp (Fig. 2 b) was created that connected the correction to lake Thun. This ramp mirrors the relief of the existing topography (slope = 8°). The elevation of lake Thun (557 m) was added to the DEM at the location of the lake shoreline before the correction was constructed and the delta developed. The lake elevation chosen is similar to the shallow bathymetric conditions existing north of the present-day delta. Within the model the lake was set as a non-erodible plane and the northernmost edge of the DEM is an open boundary where water and sediment can exit the model domain. In

the model no bedrock underlies the river channel and landscape so simulated erosion is not limited by the presence of bedrock. This this model setup is justifiable because there is no evidence (e.g. exposed bedrock) that bedrock has limited the incision of the Kander river within the modelled domain. Lastly, to encourage flow into the Kander correction at the beginning of the simulation a 3 m high barrier was created across the original channel of the Kander river.

2.4 Model outputs and test data

Model outputs consisted of 12 DEMs collected every month for the 10 years after the Kander deviation was implemented and corresponded to the years 1714-1724. Annual DEMs of difference (pre Kander correction DEM - simulated year DEM) were produced to map and analyze channel changes and the development of a delta in the lake. Channel longitudinal profiles, at 10 m spacing, were extracted from the thalweg of each annual DEM and a present-day DEM. Profiles were used to identify knickpoints by calculating the change in channel slope every 100 m. Per profile, the most upstream change in channel slope $\geq 1^\circ$ was considered the location of a knickpoint. The simulated delta consisted of deposition in the lake ≥ 2 m above the lake level (557 m) and is similar to the elevation of deposits comprising the outer, lakeward boundary of the present-day delta. For the delta, annual DEMs of difference were mapped to visualize changes in the delta topography and delta extents were delineated where simulated deposits were ≥ 2 m. Additionally, a 500 m long profile on the delta, at 10 m spacing, was taken from the simulated DEMs annually and a present-day DEM. The profile on the delta commences at the delta apex and terminates at the northern delta fringe. The location of the profile was chosen to sample topography on the delta that more than likely has not undergone major anthropogenic changes (e.g. gravel extraction). The occurrence of simulated

avulsions (i.e. rapid channel switching) on the delta were identified from deposition and erosion patterns discerned from monthly DEMs of difference.

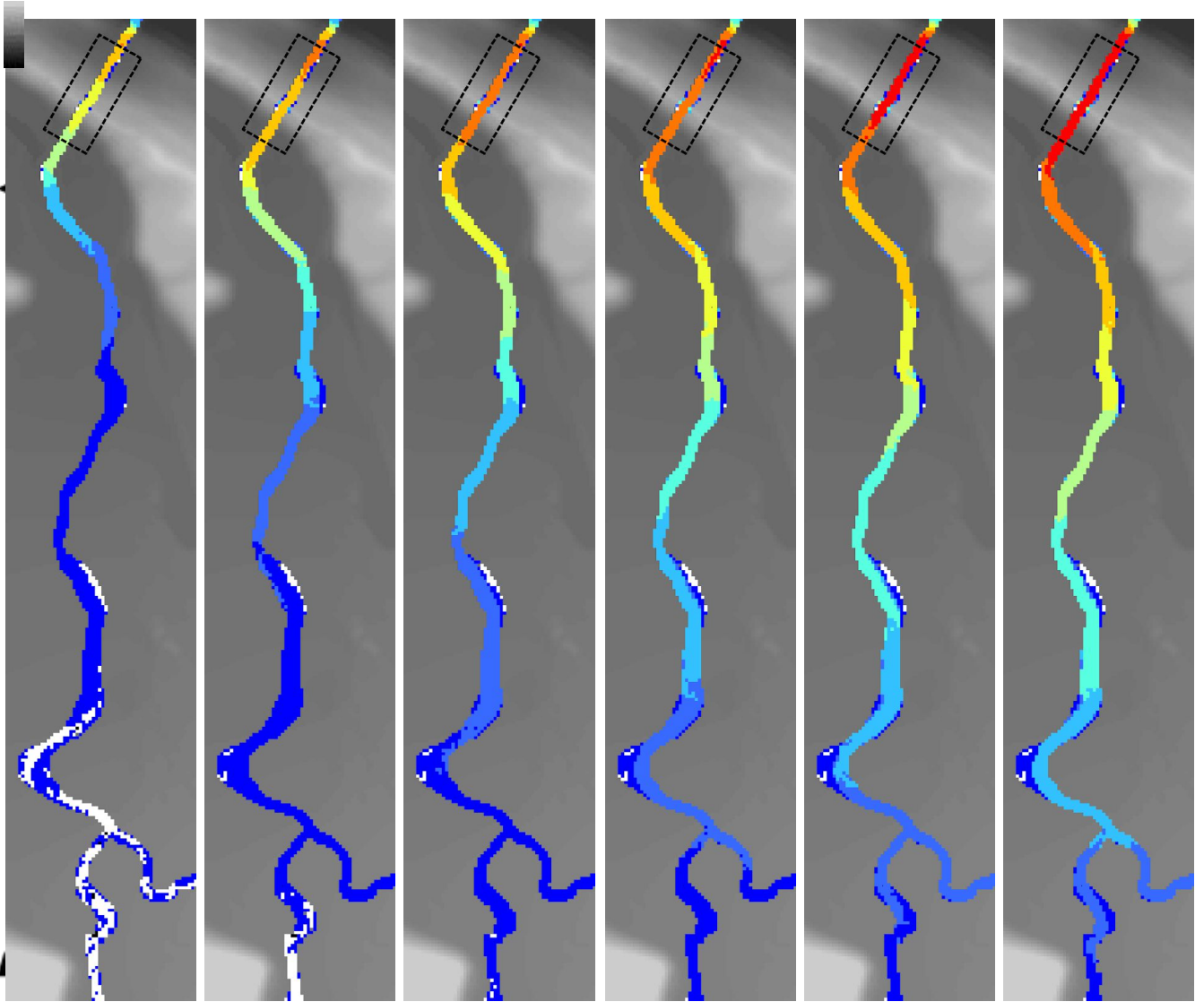
Three types of historical observations were collected to gauge the performance of CL. This data included amounts of channel erosion reported by Koch (1826) (Table 1, Fig. 2 b), knickpoint location, and delta spatial extent extracted from a georeferenced historical map (Table 1, Fig. 1 c) (Riediger, J.A., 1716). All observations represent the state of the river and delta approximately two years after the Kander was deviated (1716). These observations were compared to model output from year two and the simulated year producing the lowest combined error across all observation types. Percent error was used to determine agreement between observed and simulated erosion and knickpoint location. The agreement between simulated and observed delta extents was determined using the F measure of fitness (Bates and De Roo, 2000), which is the ratio between the intersection of observed and simulated extents, and union of observed and simulated extents. An adjusted measure (F_{adj}) was developed by bringing F to the same scale as percent error (0-100%). This adjustment was made by apply the following calculation: $F_{adj} = 100 - (F * 100)$, where $F_{adj} = 0\%$ is a perfect match between observed and simulated delta extents. This adjustment made it possible to combine percent error with F_{adj} and estimate a total error across all observation types as a Weighted Mean Percentage Error (WMPE), with equal weights per observation type.

3. Results

3.1 Channel changes

Overall, simulated channel change was dominated by erosion that propagates rapidly upstream (Fig. 3 a-h). In nine years after the Kander deviation, the model suggested

location	observed	simulated		error (%)	
	year 2	year 2	year 6	year 2	year 6
	channel erosion (m)			channel	
Kander correction	27	21.6	26.9	20	0.2
Kander river	21.6	9.5	19.8	56	8
Simme river	5.1	0.2	4.7	96	8
	knickpoint distance from Kander correction (m)			knickpoint	
Kander river	1250	1090	—	13	—
	delta spatial extent (m ²)			delta	
Kander delta	209,267	111,500	300,600	49	39
			WMPE =	40	22



-0.001 - -3

-3 - -6

-6 - -9

-9 - -12

-12 - -15

-15 - -18

-24 - -28

-21 - -24

-18 - -21

channel
change (m)

obs. erosion

Kander correction
tunnel

knickpoint

.001 - .3

.3 - .6

800

566

elevation (m)

modelled

observed

N

b)

c)

d)

e)

f)

g)

h)

Kander

Simme

Strättligen

flow

200 m

a)

year 2

year 3

year 4

year 5

year 6

year 7

year 9

year 1

Figure 3. (a-h) Channel changes (simulated year DEM - pre Kander correction DEM).

The model underestimated the year two channel erosion (Table 1), specifically at the locations in the mid-stream Kander and Simme rivers (Fig. 3 b). Mean percentage error for the model in year two was 57%, but model mean percentage error substantially decreases to 5% when observations are compared to simulated channel changes from year six (Table 1, Fig. 3 f). For the remainder of this study, in addition to considering year two model output, year six model output is used to gauge the model performance. Year six model output was chosen not because it produces the lowest model error for a specific observation type but results in the lowest combined model error across all observation types (Table 1).

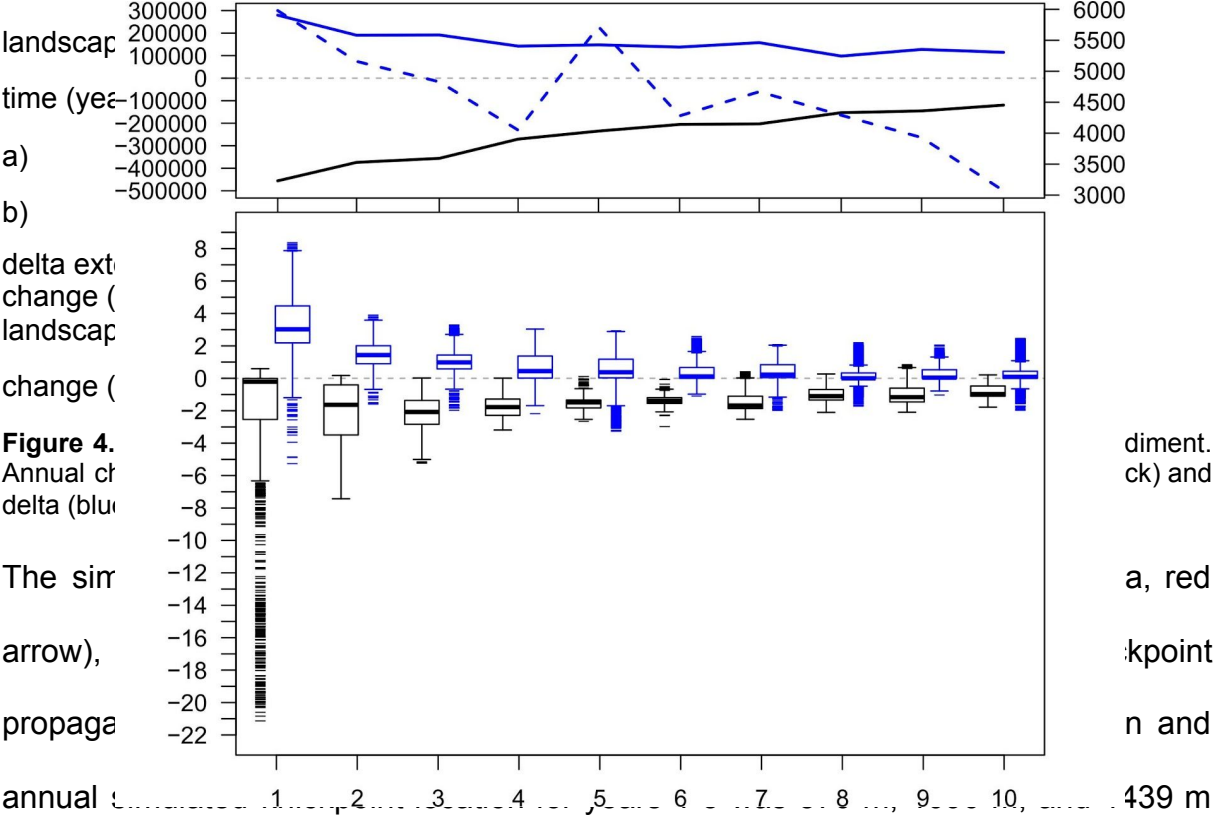
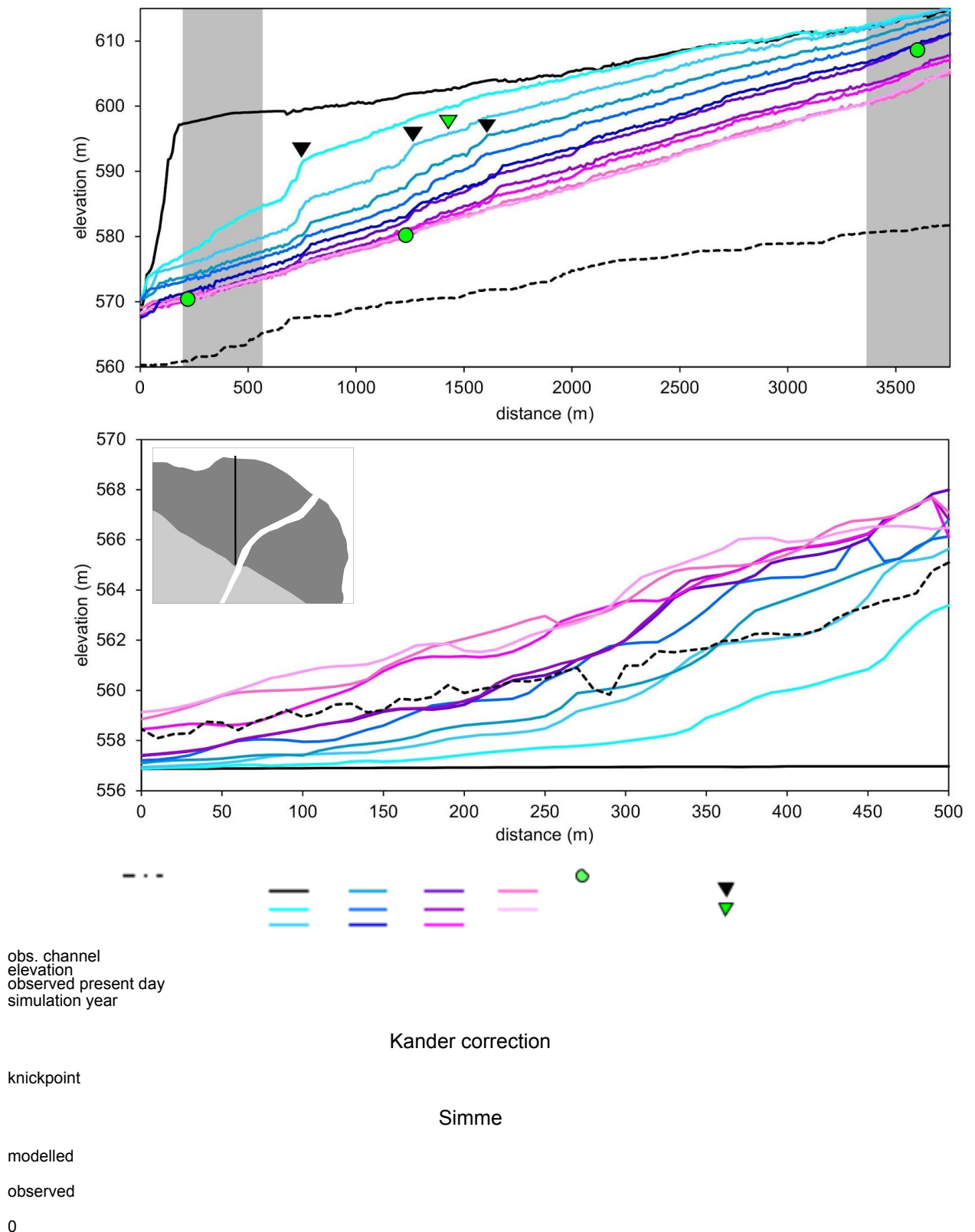


Figure 4. Annual change of delta (blue arrow), The simulation (red arrow), propagation (black arrow) and annual change (black arrow) and

respectively (Fig. 3 a-c, 5 a). The model replicates the location of the observed year two knickpoint reasonably well. At year two, the modelled knickpoint is 180 m downstream from the observed knickpoint (Fig. 3 b, 5 a), and this represents a 13% error between the observed and simulated location of the knickpoint (Table 1). Upon year four the modelled knickpoint dissipates. The dissipation of the knickpoint is

incorrectly predicted because the present-day knickpoint continues to exist but is approximately 5 km upstream in the Kander river. Importantly, the channel profiles for all years do not present evidence of erratic erosion or deposition (Fig. 5 a).



1

2

3

4

5

6

7

8

a)

b)

9

10

A

A

B

B

Kander delta

Figure 5. Longitudinal (a) channel and (b) delta profiles. Red arrow indicates initial change in river base level.

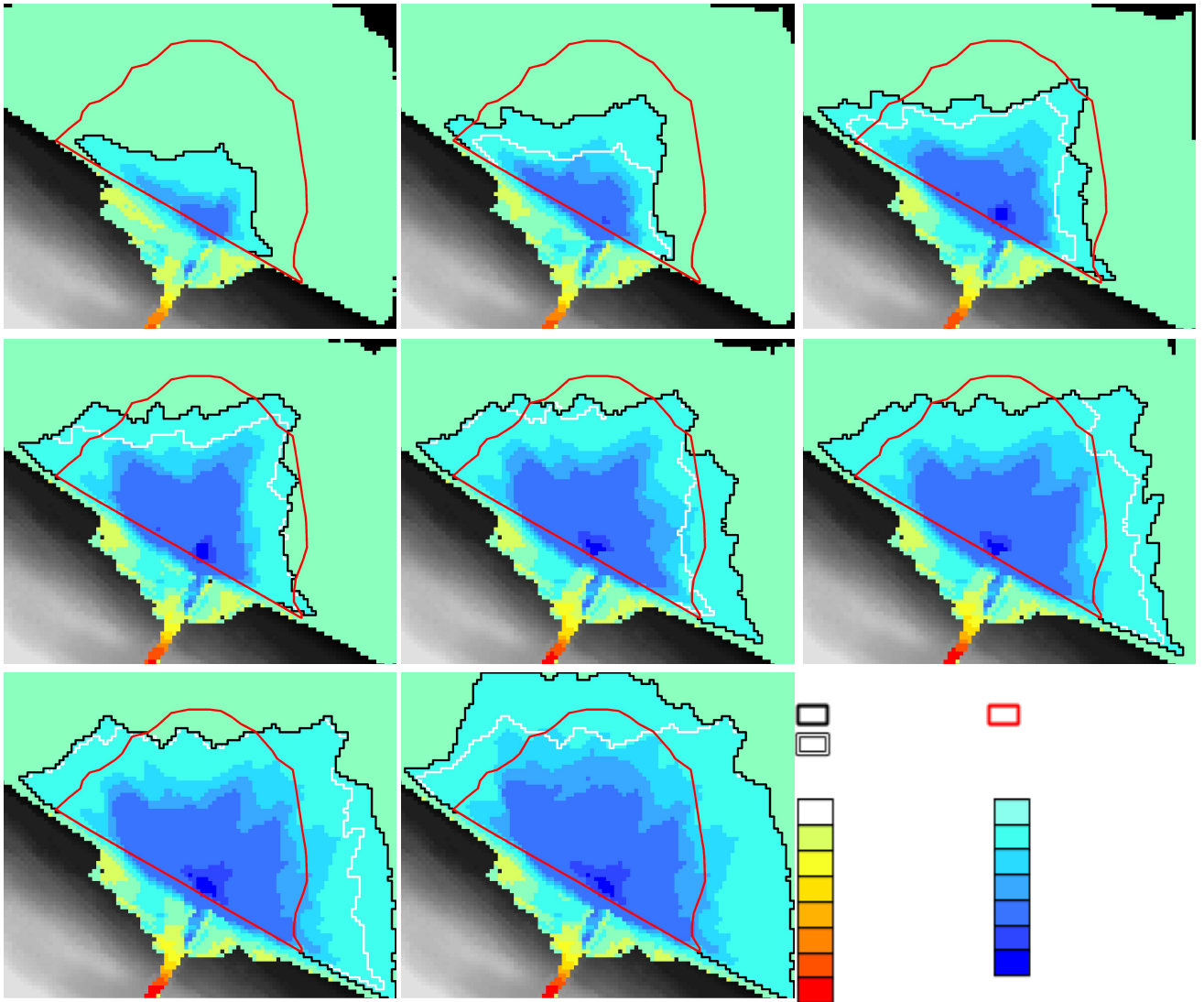
3.2 Delta formation

Delta deposits and formation mirrors the rate of channel erosion upstream (Fig. 4 a).

The model estimates that in ten years 1,587,956 m³ of sediment was deposited in the delta, with 60% of the delta forming in the first five years (Fig. 4 a). During the first year, delta deposits were mostly between 2-4.5 m, with extreme amounts of

deposition reaching 8 m, and locations of erosion occurring in the upper delta within the river channel (Fig. 4 b). In the following four years deposition in the delta steadily decreases, with most values between 0.1-2 m and delta deposition stabilizing in the remaining five years (Fig. 4 b). Throughout all simulated years, locations of erosion on the delta (e.g. year five, Fig. 4 b) are the result of avulsions that direct flow to new, readily erodible locations on the delta.

Years 1-3 delta aggradation and extent (Fig. 6 a-c) indicate the deposition of sediment across the delta is uniform in space. During this time, the delta does not exert a major control on the channel incision upstream, instead incision is mostly caused by the initial change in river base level (Fig. 5 a, red arrow). Afterwards (years 4-10), the location of delta aggradation and extent growth is controlled by avulsions that feed sediment to portions of the delta (Fig 7 a-e). Simulated avulsions develop when: 1) deposition occurs at the mouth of the delta channel (Fig. 7 a), channel slope decreases due to progradation and in-channel deposition that propagates upstream (Fig. 7 b), 3) disperse flooding over the delta occurs to search for a new channel (Fig. 7 c,d), and 4) channel switching transpires at the delta apex and flow is concentrated into the newly selected channel (Fig. 7 e) (Reitz et al., 2010). For example, from year four to five the direction of delta expansion indicates that river flow switches from north to east (Fig. 6 d,e) and delivers sediment exclusively to the eastern part of the delta. This avulsion or series of avulsions produces a 41% increase in the delta extent growth at year five (Fig. 4 a).



- year 1
- year 2
- year 3
- year 4
- year 5
- year 6
- year 7
- year 9

Lake Thun

N

modelled
delta extent

125 m

observed year 2

-0.001- -4

-4 - -8

-8 - -12

-12 - -16

-24 - -27

-20 - -24

-16 - -20

landscape change (m)

0.001- -0.001

0.001- 2

2 - 4

4 - 5

5 - 6

11 - 11.5

10 - 11

6 - 10

modelled (t -1)

Strättligen

b)

a)

c)

d)

e)

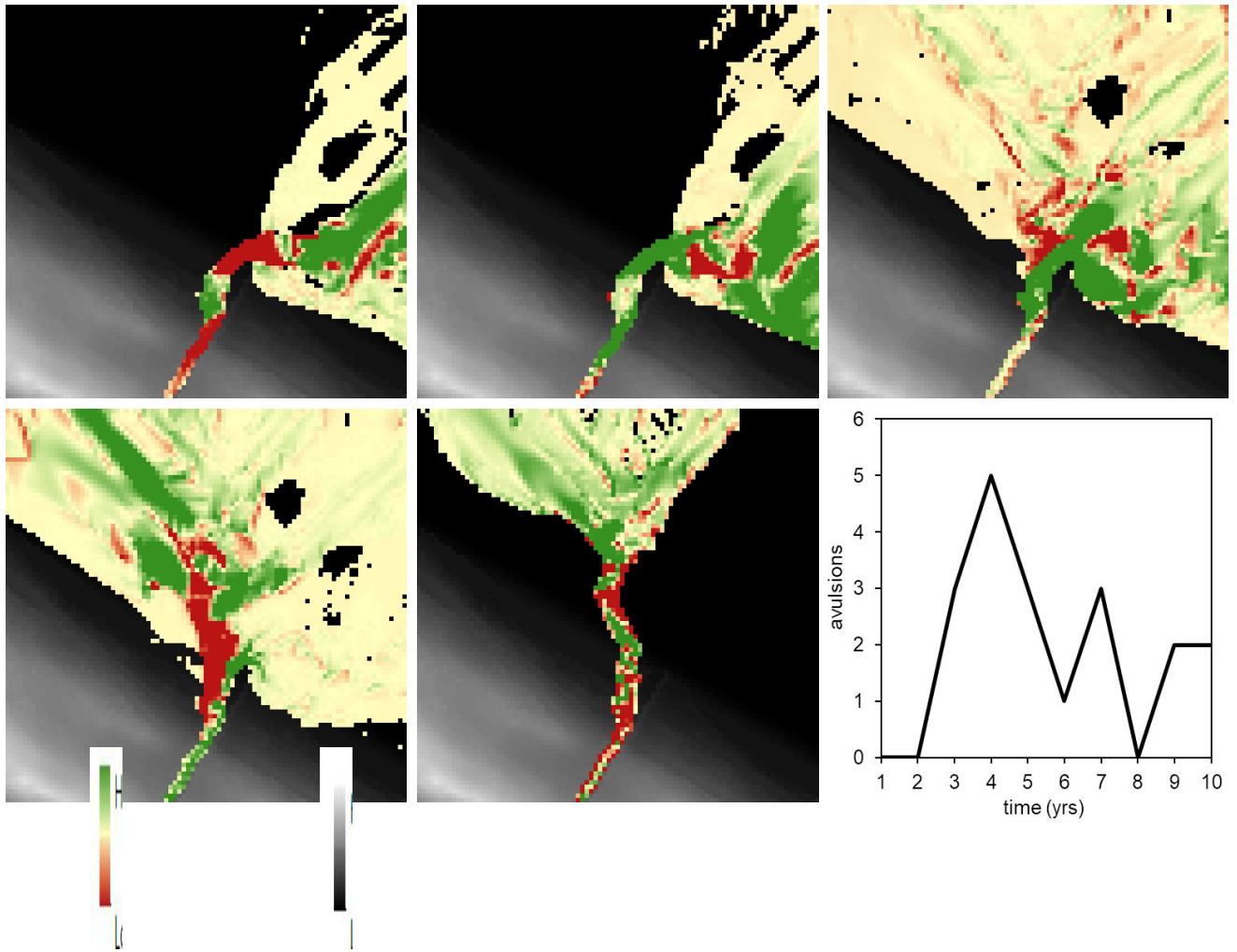
f)

g)

h)

Figure 6. (a-h) Delta formation (simulated year DEM - pre Kander delta DEM). Note that deposition in the lake < 2 m is subaqueous (green shading).

In total, 19 avulsions occurred, with no avulsions in years 1-2 when the delivery of sediment across the delta was uniform (Fig. 7 e). Avulsions commenced on year three when a discernable channel forms on the delta. Following this period, years 4-10, the frequency of avulsions is dependent on a local feedback between the upstream channel and downstream delta. The feedback transpires in the following way: 1) an avulsion occurs, 2) base level decreases, 3) channel incision upstream increases, 4) more sediment is transported downstream and 5) a new avulsion is triggered. Model results suggest that this feedback occurs in the initial period (< 10 yrs) of delta formation when locations of low elevation exist on the delta and these locations can become the base level of the river. Additionally, the occurrence of avulsions and the resulting upstream channel incision (Fig. 7 a-e) is a temporary process (< 1 yr).



Strättligen

t = 0

t = 3

t = 8

t = 9

t = 11

c)

d)

e)

f)

-1.6
1.5
landscape change (m)
elevation (m)
556
668

Figure 7. (a-e) Simulated landscape changes during an avulsion occurring on the delta commencing on the third month of year seven ($t = 0$) and with a duration of 12 months. Each image represents landscape changes occurring over one month. Negative values are erosion and positive values deposition, arrows indicate direction of flow, and elapsed time unit of measure is months. (f) Time-series of simulated avulsions occurring on delta.

Regarding model performance in replicating the delta, the year two delta spatial extent is substantially underestimated by the model and produced a $F_{adj} = 49\%$ (Fig. 6 b, Table 1). Simulated year six delta spatial extent marginally overestimated the eastern part of the observed delta extent (Fig. 6 f) but decreased error to $F_{adj} = 39\%$ (Table 1). Although the delta was formed in a short period of time with high rates of aggradation, the profile on the delta (Fig. 5 b) indicates that the model is developing a prograding delta in an expected manner with no evidence of computational instabilities that would produce anomalous patterns on the landscape. The profile also indicates that modelled delta aggradation from years 1-10 may be overestimated when compared to present-day elevations.

3.3 Overall model performance

The performance of the model in replicating year two geomorphic conditions was low, with a moderate amount of error across all observation types ($WMPE = 42\%$) (Table 1). The major contributors to model error for year two was the underestimation of: 1) the channel erosion at the two locations upstream from the Kander correction and 2) spatial extent of the delta. Model performance increases considerably when considering model output from year six against the channel erosion and delta extent observations ($WMPE = 22\%$) but omitting error stemming from the knickpoint location

because the model did not produce a knickpoint in year six. Decrease in year six error is attributed to the near replication of channel erosion at all observed locations (Table 1).

4. Discussion and study limitations

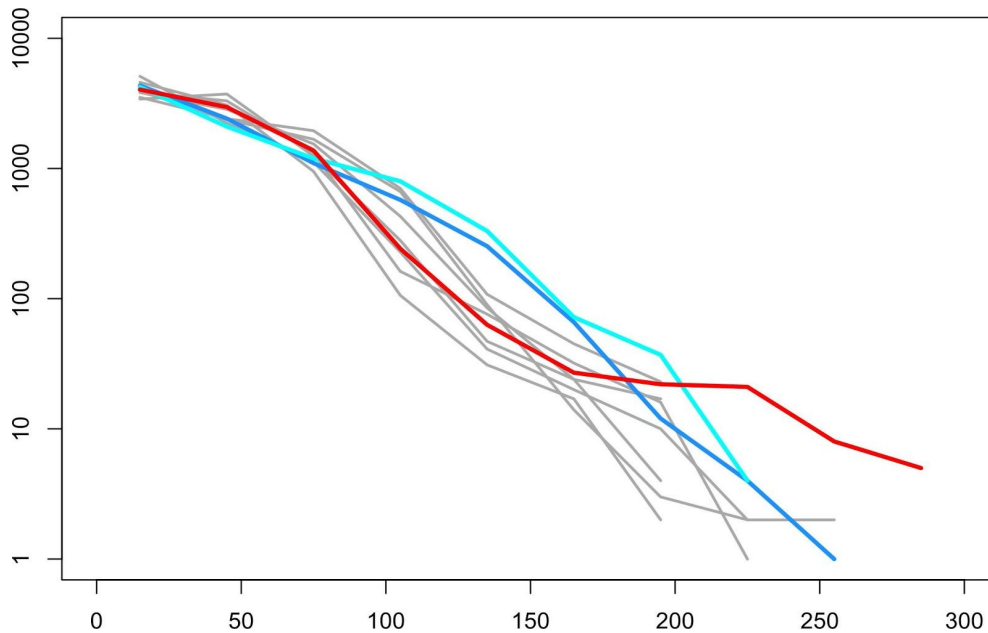
The modelling exercise shows that CAESAR-Lisflood (CL) can simulate the geomorphic response to an anthropogenic intervention to the fluvial system via a river deviation. This deviation generates high energy flows producing massive landscape changes and is a test case of CL under extreme geomorphic conditions. CL reproduced well the observed channel incision and delta extent, but with a delay of four years. In addition, comparison with observations suggested that CL simulates a stable and physically plausible replication of both erosion and deposition in the system. These results underscore the relative robustness of CL to simulate complex interactions between channel erosion, sediment supply and base level changes caused by the deposition of material in the delta. In our study, it is interesting to note that despite large uncertainties associated with sediment transport equations in Landscape Evolution Models (LEMs) (Skinner et al., 2018) and the complexity of the situation modelled, there is a good correspondence between model output and observations.

The results of our study additionally highlight the importance of modelling large sections of geomorphic systems that include connectivity between upstream (e.g. catchments and reaches) and downstream (deltas) locations. Traditionally in LEMs, importance is placed on the effect of upstream processes (e.g. hillslope erosion) and forcings (e.g. climate, land cover change) on downstream responses (e.g. sediment yield, channel change) (Wohl et al., 2019). In contrast, here we provide a case where

downstream processes exert control on upstream responses in the channel. First, the initial change in base level downstream from the Kander correction produces a knickpoint that rapidly propagates upstream and produces massive amounts of channel erosion. Second, a feedback exists whereby the occurrence of avulsions on the delta provide opportunities to lower the base level of the river and further promotes erosion upstream. Although, this feedback has been repeatedly replicated in numerical models for deltas (Geleynse et al., 2011; Liang et al., 2015; Moodie et al., 2019; Seybold et al., 2007), few if any studies have considered the effect of delta avulsions on upstream river channels. Here we recommend that delta modellers extend their area of interest inland and perform studies considering the effect of avulsions on river channel morphology upstream. Priority should be to simulate deltas responding to sea level rise through aggradation via avulsions and determine changes to upstream river morphology that expose inland communities to more flooding (Ibáñez et al., 2014; Jerolmack, 2009).

The simulation of the Kander delta formation was limited to 10 years because CL does not contain processes needed to replicate long-term delta formation (100 years) and during the simulated period (1714-1724) the Kander delta morphology was not altered significantly by humans. Although CL replicates some deltaic processes (e.g. avulsions) and provides insights into delta formation, CL is not a deltaic model and does not include processes replicating: 1) destabilization of the subaqueous delta slopes and 2) cohesiveness of delta sediment. All these processes affect deltaic long-term aggradation and spatial extent and need to be developed in CL. In addition, longer-term comparisons to the field data are difficult due to gravel extraction on the delta which produced major topographic and bathymetric changes. An estimated 7 million m³ of gravel was mined from Kander delta between 1913-1990

(Wirth, 2008) and during this time the delta did not aggrade, but decreased in elevation (Niklaus, 1969). The gravel mining was explicitly aimed at preventing the sedimentation of the shallow lake area.



hourly discharge ($\text{m}^3 \text{s}^{-1}$)

frequency

1

year

2

5

3,4,6-10

Figure 8. Annual histograms of hourly discharge, Simme and Kander combined, used as input for CAESAR-Lisflood.

Reported overall model error was 22%, but this value is not solely model error and includes error from boundary and initial conditions. For example, we may have reconstructed the river channel topography lower and steeper than the actual

historical channel. This error may have provided more aggressive channel erosion and a lower elevation from which channel erosion commenced. As such, model results matched historical observations in a shorter period. In contrast, the discharge chosen to drive CL may not be completely representative of the hydrological conditions during the Kander deviation. The proxy discharge used as model input may underestimate high flows and this reduces the rate of erosion in the model. Figure 8 helps explain the four-year delay in CL predicting observed channel erosion documented two years after the Kander deviation. Although the year one and two discharge used to drive CL contains many instances of moderately high flows ($100\text{-}200\text{ m}^3\text{ s}^{-1}$) there is low occurrence ($n = 9$) of higher flows ($> 200\text{ m}^3\text{ s}^{-1}$) that can transport more sediment (Fig. 8). Discharge from year five contains (Fig. 8) many instances of higher flow ($n = 34$) and commencing the model with this discharge would result in greater channel erosion and more than likely reduce the two-year channel erosion model error (see supplemental material for information about CL's sensitivity to hydrological inputs). CL's potential sensitivity to hydrological inputs emphasizes a need to further constrain boundary conditions. We recommend that modelling studies replicating historic landscape changes reduce uncertainty in hydrological inputs by applying methods to reconstruct trends in historic river discharge (Carson and Munroe, 2005; Evin et al., 2019) and use this information when selecting proxy hourly discharge to drive their LEMs.

Historical observations, from each type, have error that potentially increases or decreases the reported model error. For example, the delta extent was derived from a historical map that depicts landforms with less accuracy than present-day maps. This map may overestimate or underestimate the historical delta extent which may either increase or decrease model error. Likewise, the historical observations of

channel erosion contain measurement error that will affect model error. With no means to quantify and reduce the sources of error from boundary conditions, initial conditions and historical observations the reported model error remains uncertain.

5. Conclusions

We conclude that CAESAR-Lisflood (CL) shows promising results and may be useful for modelling the unintended geomorphic effects of anthropogenic interventions in river systems. Regarding our three research questions, we found: 1) CL can adequately replicate channel erosion and knickpoint propagation resulting from the Kander deviation; 2) CL can replicate the short-term (<10 yrs) development of a lake delta resulting from the Kander deviation; and 3) CL remains stable in extreme geomorphic conditions. This study provides evidence that CL could be used to predict the consequences of human interventions that include river widening, river diversions, dam removals, and river restoration efforts. CL can also be part of model chains simulating the behavior of coupled human and natural systems (Hossain et al., 2020). Such tools are required for studying the evolution of increasingly human-dominated landscapes of the Anthropocene as indicated in Verstraeten (2014).

References

- Bates, P.D., De Roo, A.P.J., 2000. A simple raster-based model for flood inundation simulation. *Journal of Hydrology* 236, 54–77.
- Bates, P.D., Horritt, M.S., Fewtrell, T.J., 2010. A simple inertial formulation of the shallow water equations for efficient two-dimensional flood inundation modelling. *Journal of Hydrology* 387, 33–45.
- Benito, G., Hudson, P.F., 2010. Flood hazards: the context of fluvial geomorphology, *Geomorphological hazards and disaster prevention*. Cambridge, Cambridge University Press.
- Best, J., 2019. Anthropogenic stresses on the world's big rivers. *Nature Geoscience* 12, 7–21.
- Bhuyian, M.N., Kalyanapu, A., Hossain, F., 2017. Evaluating conveyance-based DEM correction technique on NED and SRTM DEMs for flood impact assessment of the 2010 Cumberland river flood. *Geosciences* 7, 132.

- Bögli, T., 2018. Der prägende Einfluss der Kander auf die Region Thun. Werd Weber Verlag AG.
- Brown, A.G., Tooth, S., Bullard, J.E., Thomas, D.S., Chiverrell, R.C., Plater, A.J., Murton, J., Thorndycraft, V.R., Tarolli, P., Rose, J., 2017. The geomorphology of the Anthropocene: emergence, status and implications. *Earth Surface Processes and Landforms* 42, 71–90.
- Bütschi, D., 2008. Gefürchtet, gebändigt und neu gedacht – die Kander. Die Geschichte eines Flusses und seiner Menschen (1800-1950). Historisches Institut der Universität Bern., Bern.
- Carson, E.C., Munroe, J.S., 2005. Tree-ring based streamflow reconstruction for Ashley Creek, northeastern Utah: implications for palaeohydrology of the southern Uinta Mountains. *The Holocene* 15, 602–611.
- Coulthard, T.J., Macklin, M.G., Kirkby, M.J., 2002. A cellular model of Holocene upland river basin and alluvial fan evolution. *Earth Surface Processes and Landforms* 27, 269–288.
- Coulthard, T.J., Neal, J.C., Bates, P.D., Ramirez, J., de Almeida, G.A.M., Hancock, G.R., 2013. Integrating the LISFLOOD-FP 2D hydrodynamic model with the CAESAR model: implications for modelling landscape evolution. *Earth Surface Processes and Landforms* 38, 1897–1906.
- Coulthard, T.J., Skinner, C.J., 2016. The sensitivity of landscape evolution models to spatial and temporal rainfall resolution. *Earth Surface Dynamics* 4, 757.
- Culmann, K., 1865. Rapport au Conseil fédéral sur les torrents des Alpes suisses inspectés en 1858, 1859, 1860 et 1863. L. Corbaz.
- Di Baldassarre, G., Kreibich, H., Vorogushyn, S., Aerts, J., Arnbjerg-Nielsen, K., Barendrecht, M., Borga, M., Bates, P., Borga, Marco, Botzen, W., 2018. An interdisciplinary research agenda to explore the unintended consequences of structural flood protection. *Hydrology and Earth System Sciences* 22, 5629–5637.
- Evin, G., Wilhelm, B., Jenny, J.-P., 2019. Flood hazard assessment of the Rhône River revisited with reconstructed discharges from lake sediments. *Global and Planetary Change* 172, 114–123.
- Feeney, C.J., Chiverrell, R.C., Smith, H.G., Hooke, J.M., Cooper, J.R., 2020. Modelling the decadal dynamics of reach-scale river channel evolution and floodplain turnover in CAESAR-Lisflood. *Earth Surface Processes and Landforms* 45, 1273–1291.
- FOEN, 2020. Federal Office for the Environment Switzerland: Hydrologic data of Bern [WWW Document]. URL www.hydrodaten.admin.ch
- Fortugno, D., Boix-Fayos, C., Bombino, G., Denisi, P., Quiñonero Rubio, J.M., Tamburino, V., Zema, D.A., 2017. Adjustments in channel morphology due to land-use changes and check dam installation in mountain torrents of Calabria (southern Italy). *Earth Surface Processes and Landforms* 42, 2469–2483.
- Geleynse, N., Storms, J.E., Walstra, D.-J.R., Jagers, H.A., Wang, Z.B., Stive, M.J., 2011. Controls on river delta formation; insights from numerical modelling. *Earth and Planetary Science Letters* 302, 217–226.
- Gregory, K.J., 2006. The human role in changing river channels. *Geomorphology* 79, 172–191.
- Grosjean, G., 1962. Die Ableitung der Kander in den Thunersee vor 250 Jahren, in: *Jahrbuch Des Thunerund Brienersee. Interlaken*, pp. 18–40.
- Hancock, G.R., Duque, J.M., Willgoose, G.R., 2019. Geomorphic design and modelling at catchment scale for best mine rehabilitation—The Drayton mine example (New South Wales, Australia). *Environmental Modelling & Software* 114, 140–151.
- Hinderer, M., 2001. Late Quaternary denudation of the Alps, valley and lake fillings and modern river loads. *Geodinamica Acta* 14, 231–263.
- Hooke, R.L., 2000. On the history of humans as geomorphic agents. *Geology* 28, 843–846.
- Hossain, M.S., Ramirez, J.A., Haisch, T., Speranza, C.I., Martius, O., Mayer, H., Keiler, M., 2020. A coupled human and landscape conceptual model of risk and resilience in Swiss Alpine communities. *Science of the Total Environment* 138322.
- Ibáñez, C., Day, J.W., Reyes, E., 2014. The response of deltas to sea-level rise: natural mechanisms and management options to adapt to high-end scenarios. *Ecological Engineering* 65, 122–130.

- James, L.A., Marcus, W.A., 2006. The human role in changing fluvial systems: Retrospect, inventory and prospect. *Geomorphology* 79, 152–171.
- Jerolmack, D.J., 2009. Conceptual framework for assessing the response of delta channel networks to Holocene sea level rise. *Quaternary Science Reviews* 28, 1786–1800.
- KAWA, 2015. Kantons Bern: LiDAR Bern – Airborne Laserscanning. Gesamtbericht Befliegung – Befliegung Kanton Bern 2011 – 2014. KAWA Amt für Wald des Kantons Bern.
- Koch, C.I.I., 1826. Bericht der Schwellen-Commission ... über die Correktion der Aar von Thun bis Bern. Staingsli.
- Liang, M., Voller, V.R., Paola, C., 2015. A reduced-complexity model for river delta formation-Part 1: Modeling deltas with channel dynamics. *Earth Surface Dynamics* 3, 67–86.
- Liu, B., Coulthard, T.J., 2017. Modelling the interaction of aeolian and fluvial processes with a combined cellular model of sand dunes and river systems. *Computers & Geosciences* 106, 1–9.
- Lowry, J.B.C., Narayan, M., Hancock, G.R., Evans, K.G., 2019. Understanding post-mining landforms: Utilising pre-mine geomorphology to improve rehabilitation outcomes. *Geomorphology* 328, 93–107.
- Marsh, G.P., 1864. *Man and Nature*. Sampson Low, Son and Marston, New York.
- Moodie, A.J., Nittrouer, J.A., Ma, H., Carlson, B.N., Chadwick, A.J., Lamb, M.P., Parker, G., 2019. Modeling deltaic lobe-building cycles and channel avulsions for the Yellow River delta, China. *Journal of Geophysical Research: Earth Surface* 124, 2438–2462.
- Munoz, S.E., Giosan, L., Therrell, M.D., Remo, J.W., Shen, Z., Sullivan, R.M., Wiman, C., O'Donnell, M., Donnelly, J.P., 2018. Climatic control of Mississippi River flood hazard amplified by river engineering. *Nature* 556, 95–98.
- Niklaus, M., 1969. Die Kander und ihr Delta im Thunersee. *Jahrbuch vom Thuner- und Brienersee, Interlaken*.
- Nunnally, N.R., Keller, E., 1979. Use of fluvial processes to minimize adverse effects of stream channelization. Water Resources Research Institute of the University of North Carolina.
- Pasculli, A., Audisio, C., 2015. Cellular automata modelling of fluvial evolution: real and parametric numerical results comparison along River Pellice (NW Italy). *Environmental Modeling & Assessment* 20, 425–441.
- Poeppl, R.E., Coulthard, T., Keesstra, S.D., Keiler, M., 2019. Modeling the impact of dam removal on channel evolution and sediment delivery in a multiple dam setting. *International Journal of Sediment Research* 34, 537–549.
- Ponce, V.M., 1989. *Engineering hydrology: Principles and practices*. Prentice Hall Englewood Cliffs, NJ.
- Reitz, M.D., Jerolmack, D.J., Swenson, J.B., 2010. Flooding and flow path selection on alluvial fans and deltas. *Geophysical Research Letters* 37.
- Riediger, J.A., 1716. Kander, unterer Lauf nach 1711: Plan des neuen Kanderkanals (Kanderdurchstich) und des alten Laufs der Kander samt Gegend von Thun, mit Grundriss Bälliz (Thun).
- Röthlisberger, G., 1991. *Chronik der Unwetterschäden in der Schweiz*. Eidgenössische Forschungsanstalt für Wald Schnee und Landschaft.
- Schlunegger, F., Hinderer, M., 2003. Pleistocene/Holocene climate change, re-establishment of fluvial drainage network and increase in relief in the Swiss Alps. *Terra Nova* 15, 88–95.
- Seybold, H., Andrade, J.S., Herrmann, H.J., 2007. Modeling river delta formation. *Proceedings of the National Academy of Sciences* 104, 16804–16809.
- Tiefbauamt des Kantons Bern, 2004. Amt für Landwirtschaft und Natur des Kantons Bern (2004) Geschiebehalt Kander.
- Triet, N.V.K., Nguyen, V.D., Fujii, H., Kummu, M., Merz, B., Apel, H., 2017. Has dyke development in the Vietnamese Mekong Delta shifted flood hazard downstream? *Hydrology and Earth System Sciences* 21, 3991.

- Tucker, G.E., Hancock, G.R., 2010. Modelling landscape evolution. *Earth Surface Processes and Landforms* 35, 28–50.
- Van De Wiel, M.J., Coulthard, T.J., Macklin, M.G., Lewin, J., 2007. Embedding reach-scale fluvial dynamics within the CAESAR cellular automaton landscape evolution model. *Geomorphology* 90, 283–301.
- Verstraeten, G., 2014. Quantification of human-environment interactions in the past. *Anthropocene* 8, 1–5.
- Vischer, D.L., 2004. Die Geschichte des Hochwasserschutzes in der Schweiz. Von den Anfängen bis ins 19. Jahrhundert. *Schweiz. Z. Forstwes* 155, 517–518.
- Walsh, P., Jakeman, A., Thompson, C., 2020. Modelling headwater channel response and suspended sediment yield to in-channel large wood using the Caesar-Lisflood landscape evolution model. *Geomorphology* 107209.
- Wilcock, P.R., Crowe, J.C., 2003. Surface-based transport model for mixed-size sediment. *Journal of Hydraulic Engineering* 129, 120–128.
- Willgoose, G., Riley, S., 1998. The long-term stability of engineered landforms of the Ranger Uranium Mine, Northern Territory, Australia: application of a catchment evolution model. *Earth Surface Processes and Landforms* 23, 237–259.
- Wirth, S., 2008. Lake Thun sediment record: 300 years of human impact, flood events and subaquatic slides. Federal Institute of Technology ETH, Department of Earth Sciences.
- Wirth, S.B., Girardclos, S., Rellstab, C., Anselmetti, F.S., 2011. The sedimentary response to a pioneer geo-engineering project: Tracking the Kander River deviation in the sediments of Lake Thun (Switzerland). *Sedimentology* 58, 1737–1761.
- Wohl, E., 2006. Human impacts to mountain streams. *Geomorphology* 79, 217–248.
- Zambrano-Bigiarini, M., 2012. HydroTSM: Time series management, analysis and interpolation for hydrological modelling. R package version 0.3 3.
- Ziliani, L., Surian, N., Botter, G., Mao, L., 2020. Assessment of the geomorphic effectiveness of controlled floods in a braided river using a reduced-complexity numerical model. *Hydrology and Earth System Sciences* 24, 3229–3250. <https://doi.org/10.5194/hess-24-3229-2020>
- Zischg, A.P., Hofer, P., Mosimann, M., Röthlisberger, V., Ramirez, J.A., Keiler, M., Weingartner, R., 2018. Flood risk (d) evolution: Disentangling key drivers of flood risk change with a retro-model experiment. *Science of the Total Environment* 639, 195–207.